

Contents lists available at [ScienceDirect](http://ScienceDirect.com)

## Energy Reports

journal homepage: [www.elsevier.com/locate/egy](http://www.elsevier.com/locate/egy)

## Research paper

## Solar PV energy system in Malaysian airport: Glare analysis, general design and performance assessment

S. Sreenath <sup>a,d</sup>, K. Sudhakar <sup>b,c,d,\*</sup>, Yusop A.F. <sup>b</sup>, E. Solomin <sup>d</sup>, I.M. Kirpichnikova <sup>d</sup><sup>a</sup> Renewable Energy and Energy Efficiency Research Cluster, Universiti Malaysia Pahang, Malaysia<sup>b</sup> Faculty of Mechanical and Automobile Engineering Technology, Universiti Malaysia Pahang, 26600, Malaysia<sup>c</sup> Energy Centre, Maulana Azad National Institute of Technology Bhopal, India<sup>d</sup> Department of Electric stations, Grids, and Power Supply systems, South Ural State University, Chelyabinsk, Russian Federation

## ARTICLE INFO

## Article history:

Received 18 July 2019

Received in revised form 16 March 2020

Accepted 16 March 2020

Available online xxxx

## Keywords:

Airport

Glare

Performance

Photovoltaic

Solar

Simulation

## ABSTRACT

There is a growing interest in airport-based solar plant installations around the world. The buffer zone area in airports can effectively be utilized by tapping solar energy. However, it possesses concern for air safety and navigation mainly from the possible glare of the PV array. The objective of the study is to analyze the technical performance of a proposed solar PV plant in the premises of Kuantan Airport, Malaysia using SolarGis software with due consideration of glare occurrence. Eight zones are selected, and it was observed that yellow glare will occur for 4,552 min at ATC from Zone 8. The impact of glare from the other zones is in accordance with FAA's glare policy. The selected zones cover 0.2677 km<sup>2</sup> of the airport's land with solar potential of 20 MW. The proposed solar PV plant consists of 57,143 crystalline silicon PV modules. Each PV string consists of PV modules of 20 in number. The number of strings in the entire PV plant is 2,857. The proposed PV plant requires 40 numbers of central inverters and 20 numbers of transformers. The proposed solar PV power plant is expected to generate 26,304 MWh annually and this energy generation is 168 times the energy consumption of the airport's terminal building. The highest energy production will be observed in March (2,514 MWh). It is projected that the monthly average final yield varies from a maximum value of 125.70 MWh/MWp-month in March to a minimum of 90.70 MWh/MWp-month in December. The proposed solar plant in Kuantan airport is expected to perform sufficiently well with 76.88 % performance ratio and 15.22 % capacity utilization factor. These results predict the safe operation of the airport-based solar system in Malaysia without glare impact.

© 2020 Published by Elsevier Ltd. This is an open access article under the CC BY-NC-ND license (<http://creativecommons.org/licenses/by-nc-nd/4.0/>).

## 1. Introduction

The aviation industry is witnessing rapid growth during the past several years. Low-cost carriers and regional airlines have revolutionized the aviation business. The aviation industry is expected to maintain positive growth for the next thirty years ([Massachusetts Institute of Technology, 2019](#)). This transport industry emits about 3% of total greenhouse gases ([United States Environmental Protection Agency, 2019](#)). Most of the airports depend on conventional power plants to meet their electrical energy requirements ([Shukla et al., 2016](#)). These power plants lead to indirect emission of greenhouse gases to the atmosphere causing pollution. The carbon footprint of the airport can be reduced by consuming electricity generated from non-polluting sources of energy such as solar, wind, biomass etc. Airport premises have

\* Corresponding author at: Energy Centre, Maulana Azad National Institute of Technology Bhopal, India.

E-mail address: [sudhakar@ump.edu.my](mailto:sudhakar@ump.edu.my) (K. Sudhakar).

recently become a favorite location for solar photovoltaic plants across the world. Solar PV modules can be installed in the land as well as integrated to rooftop or walls of buildings. Commissioning of solar plants in the airport possesses a unique challenge to solar developers ([Wybo, 2013](#)). Solar PV technologies in the airport may lead to different types of impacts such as physical penetration of airspace, radar interference, glare occurrence which in turn may affect the operation of the airport ([Barrett et al., 2014](#)).

[Anurag et al. \(2017\)](#) studied the technical barriers to the implementation of solar PV systems in an airport and reported that the glare from PV modules is one of the main roadblocks. The aviation authorities are concerned about the possible visual impairment of pilots and airport staff due to glare/glint from the proposed solar PV plant. In 2012, a section of PV array in Manchester–Boston Airport, US was covered temporarily with traps for avoiding hours of blinding glare seen at the control tower. Later on, the orientation of the PV array was changed to avoid glare strikes. These alterations reduced the energy yield from the solar plant and reported an economic loss in millions

of dollars. To avoid such situations, it is suggested to follow the guidelines of the Federal Aviation Administration (FAA) on glare impact (Ho, 2013). According to these guidelines, the project developer should prove that the PV arrays do not cause glare in the existing Airport Traffic Control (ATC) tower and glare or low potential for afterimage along the flight approach path. As of now, glare impact studies carried out by the FAA and its guidelines are considered for solar projects in airports across the world (Mostafa and Zobaa, 2016).

Song and Choi (2016) carried out the preliminary design of the floating solar PV system in pit lakes and estimated that solar energy potential was 971.57 MWh annually. There is quite a wide range of software programs available for simulating solar PV systems. Gurupira and Rix (2017) assessed the capabilities of three PV software PVSyst, SAM and PVlib in different PV modeling scenarios. The percentage difference between actual and predicted yield was 3.37% (PVSyst), 3.86% (SAM) and 5.07% (PVLib). Tiba and Barbosa de (2002) evaluated the software programs used for designing, simulation, and diagnosis of photovoltaic water-pumping systems based on four criteria. Chikh et al. (2011) discussed the sizing aspects of the new photovoltaic simulation tool. This software is intended for accuracy in the local Algerian climate and the performance results were compared with other PV software such as PVSyst and EoS 1.1 (BP Solar). Choi et al. (2011) proposed a methodology for coupling ArcGIS with TRNSYS that enables the PV Analyst extension. This allows the user to practice the capabilities of different PV array performance models and the irradiance components in TRNSYS for solar energy simulations in geospatial contexts. Siraki and Pillay (2010) compared the results of two urban application designed solar tool namely Ecotect 2010 and PVSyst 5.05 for a building in Montreal. According to them, the PVSyst software package is more suitable for the detailed design where the PV system parts are selected to obtain the highest possible energy outcome. Also, the estimated generation of electrical energy is more accurate when simulated with PVSyst than Ecotect. Lalwani et al. (2010) evaluated several solar PV software based on availability, cost, platform, capacity, scope and updatability. Sukumaran and Sudhakar (2017a) compared the real performance of 12 MW solar plant using onsite value with that predicted by SolarGis and observed that the real and predicted performance parameters such as PR, CUF match closely. In SolarGis software, highly accurate satellite data is used for simulation and offers a rigorous systematic approach. Also, it has some inbuilt features such as automatic calculation of terrain shading. SolarGis database retrieves data from 19 geostationary satellites at five principal positions, and atmospheric & meteorological models operated by renowned meteorological data centers.

Several authors carried out the performance analysis of solar PV plants using operational data (Goura, 2015; Kumar and Sudhakar, 2015; Padmavathi and Daniel, 2013; Sundaram and Babu, 2015; Verma and Singhal, 2015). Kumar and Sudhakar (2015) evaluated the performance of 10 MWp grid-tied solar photovoltaic systems in Ramagundam, India using the on-site data. The plant performed sufficiently well with an average performance ratio (PR) of 86.12% and Capacity Utilization Factor (CUF) of 17.68% during the observed period. Sundaram and Babu (2015) carried out the performance analysis of the 5 MWp grid-connected photovoltaic system in the southern part of India using plant monitored data and found that the daily averaged final yield was 4.81 hours/day with a total system efficiency of 5.08%. Padmavathi and Daniel (2013) analyzed the performance of a 3 MW grid-connected SPV plant in Karnataka, India using plant data, and concluded that the plant operates with good CUF value. Few authors worked exclusively on the performance of airport-based solar PV systems based on operational data (Banda et al., 2019; Mpholo et al., 2014; Sukumaran and Sudhakar, 2017a,b). Sukumaran and Sudhakar (2017a,b) assessed the energy performance

of the 12 MW solar PV plant installed in Cochin airport, India. It was observed that the plant is performing well with performance ratio (86.56%) and capacity utilization factor (20.12%). Banda et al. (2019) presented the performance assessment of the 830 kWp solar PV power plant at Kamuzu airport, Malawi and found that the efficiencies of PV array (15.3%), inverter (95.2%) and overall system (14.6%) for an annual four-year averaged period. Sukumaran and Sudhakar (2017a,b) carried out a feasibility study for solar PV plant in the premises of Raja Bhoja airport, India. The proposed 2 MW solar power plant is expected to produce 2733.12 MWh units of electricity annually with mean specific energy yield and performance ratio value of 113.88 kWh/kWp and 85.54% respectively. It was seen that the performance of the solar PV plant was carried out based on yield parameters, performance ratio, capacity factor, plant efficiency etc. In addition, most of the performance assessment was carried out for a solar PV plant located in the non-airport areas.

Alba and Manana (2016) analyzed the various energy aspects in the airport such as main energy sources, application of energy conservation, efficiency, energy modeling and simulation. Rubeis et al. (2016) analyzed the electrical energy, thermal energy and fuel consumption of Leonardo da Vinci International Airport, Rome based on historical data. They proposed a smart load management solutions which involve finding an optimal point between production and consumption. Rowlings (2016) presented a study on various renewable energy sources that can be implemented in the airport facilities. It was found that energy generation based on solar and cogeneration sources are more suitable as compared to other sources of energy for an airport in terms of sustainability. Somcharoenwattanaa et al. (2011) analyzed the performance of 52.5 MWe cogeneration plant at the Suvarnabhumi airport in Bangkok and reported a reduction (24%) in the primary energy use from conventional energy sources which in turn led to decrease in CO<sub>2</sub> emissions (27%). Kilkis and Kilkis (2016) analyzed a few major airports on the basis of services, quality, energy use, energy production, reduction in CO<sub>2</sub> emissions, environmental conservation and low emission transport. These authors suggested that an airport's ecological impact can be greatly influenced by switching to renewable energy. Wybo (2013) addressed safety concerns associated with the implementation of airport-based photovoltaic systems and emphasized the significance of mitigation measures to avoid risk to aviation.

From the scarce number of available literature, it was concluded that the concept of tapping solar energy from airport premises is relatively new. It was noted that only a few works reported the performance analysis of solar systems in airport conditions. In addition to that, none of these work was specific to Malaysian airport conditions.

The objectives of this study are

- To assess the glare impact from the proposed utility-scale ground-mounted solar PV system in Kuantan airport using ForgeSolar software.
- To estimate the solar photovoltaic power potential in Kuantan airport, Malaysia based on land availability and glare assessment.
- To perform the preliminary design of the proposed solar PV system in Kuantan airport, Malaysia.
- To evaluate the energy performance of the solar PV plant in Kuantan airport using SolarGis software and mathematical equations.

## 2. Methodology

A solar PV power plant is proposed in different areas within the premises of Kuantan airport. The glare impact from each site

**Table 1**  
Selected zones in Kuantan airport for the proposed PV system.

Zone	Area	
	In sq. km	In acres
Zone 1	0.029	7.167
Zone 2	0.017	4.20
Zone 3	0.056	13.95
Zone 4	0.030	7.41
Zone 5	0.043	10.62
Zone 6	0.025	6.17
Zone 7	0.067	16.55
Zone 8	0.0096	2.39

is assessed using ForgeSolar software. The performance of the solar system is analyzed using the simulated data from SolarGIS software.

### 2.1. Airport description and site selection

Sultan Ahmad Shah International Airport or Kuantan airport is located in the Pahang state of Malaysia. It serves as the Air Force base as well as the civilian airport which mainly caters to the transport of local passengers from Kuantan to Kuala Lumpur. Using the mapping tool, it was found that Kuantan airport spreads over 3.765 km<sup>2</sup> or 930.458 acres. The land footprint of Kuantan airport is shown in Fig. 1. The geographical coordinates of Kuantan airport are taken as 03°46N latitude, 103°12E longitude and has an elevation of 18 m. This airport has a single runway that is 2804 m in length and 45 m in width (Wikipedia, 2018), (Shalya, 2009). This airport has a single terminal for arrival and departure. The airport terminal has a built area of 7778 m<sup>2</sup> (Personal Communication, 2020). A visit to the airport was carried out and details such as energy consumption and location of ATC tower were collected. The monthly electrical energy consumption of the terminal building was 155,890.58 kWh for the year 2019, for which the airport had to pay an amount of 77,990.211 Malaysian Ringgit to the electricity board.

Within the premises of the airport, different zones are selected for the proposed solar PV system. The areas occupied by terminal building, other built area and runway protection zones are avoided. The summary of zone selection is given in Table 1. In the selected zones, the following assumptions are considered.

- The interference to the operation of communication systems is very low.
- The solar PV installation does not affect the airspace facilities and airspace restrictions.
- No future development activities will be scheduled for the next 30 years in the selected zone.

The glare effect from PV modules has significant impact on the safe operation of the airport. So, glare assessment is carried out for each zone with the help of a prediction tool.

### 2.2. Glare assessment using ForgeSolar

ForgeSolar software helps in the determination of the occurrence of glare from the PV system and its impact on the observer. Federal Aviation Administration (FAA) recommends the use of ForgeSolar software and suggests to obtain no glare hazard report of the proposed PV array. Only a few software is available for glare prediction. This software is developed by Sandia laboratories and is licensed to Sims industries. The default values of direct normal irradiance, PV panel reflectivity, its optical properties, ocular parameters, and orientation are used in the simulation. The glare prediction involves some assumptions and approximations such

as reflected ray parameters and observer eye properties as per FAA's glare policy. The inputs needed for each simulation are described in Table 2.

The amount of sunlight reflected from the solar PV module mainly depends on the intensity of solar irradiation, properties of PV module, size and orientation of PV array, PV technology and ocular parameters. Glare is defined as a continuous source of light. Glare occurrence can be predicted mathematically using algebraic equations. The estimation of glare from solar PV array involves several mathematical steps. Vector algebra is applied to find whether glare is seen from the given observation points. These complex mathematical computations are provided in the technical reference manual of Solar Glare Hazard Analysis Tool (SGHAT). Based on this, ForgeSolar software predicts the occurrence of glare and its hazard as per the FAA's policy on glare.

Step 1: Calculate the solar time,  $T_{solar}$  using Eq. (1)

$$T_{solar} = 4(L_{sm} - L_{lon}) + Eot + T_{std} \quad (1)$$

where  $L_{sm}$  is the local standard meridian,  $L_{lon}$  is the local longitude,  $Eot$  is the equation of time in minutes,  $T_{std}$  is the standard time

$$L_{sm} = \text{Time Zone} \times 15$$

$$\text{Equation of time, } Eot = 229.2 (0.000075 + 0.001868 \times \cos B - 0.0320077 \times \sin B - 0.014615 \times \cos 2B - 0.04089 \times \sin 2B)$$

Step 2: Hour Angle,  $A_h$  is calculated using the value of solar time ( $T_s$ ) and solar noon ( $T_n$ )

$$A_h = (T_s - T_n) \times 15 \quad (2)$$

Step 3: The value of declination,  $\delta$  is found out using Eq. (3).

$$\delta = 23.450 \times \sin \left( 360 \times \left\{ \frac{284 + n}{365} \right\} \right) \quad (3)$$

where  $n$  denotes the day of the year (1 to 365)

Step 4: The value of the zenith angle,  $\theta_z$  is found out using Eq. (4).

$$\theta_z = \cos^{-1}(\cos l \times \cos \delta \times \cos A_h + \sin l \times \sin \delta) \quad (4)$$

where  $l$  is the given local latitude

Step 5: Azimuthal angle ( $A_{az}$ ) and Altitude angle ( $A_{al}$ ) of the sun is calculated using Eq. (5).

$$A_{az} = \text{sign}(A_h) \times \left| \cos^{-1} \left( \frac{\cos \theta_z \times \sin \varphi - \sin \delta}{\sin \theta_z \times \cos \varphi} \right) \right| \quad (5)$$

$$A_{al} = (A_{az} - 90^\circ) \quad (6)$$

Step 6: The position of the sun ( $SP_i$ ,  $SP_j$ ,  $SP_k$ ) is a function of azimuthal ( $A_{az}$ ) and altitudinal angle ( $A_{al}$ ). Sun position can also be represented as a unit vector extending from the origin towards the sun.

$$\vec{SP}_i = \cos A_{al} \times \sin A_{az} \quad (7)$$

$$\vec{SP}_j = \cos A_{al} \times \cos A_{az} \quad (8)$$

$$\vec{SP}_k = \sin A_{al} \quad (9)$$

Step 7: Reflected sun vector is determined using the reflection equation based on the normal vector to the PV array (Weisstein, 2019). It also requires the knowledge of sun position for each



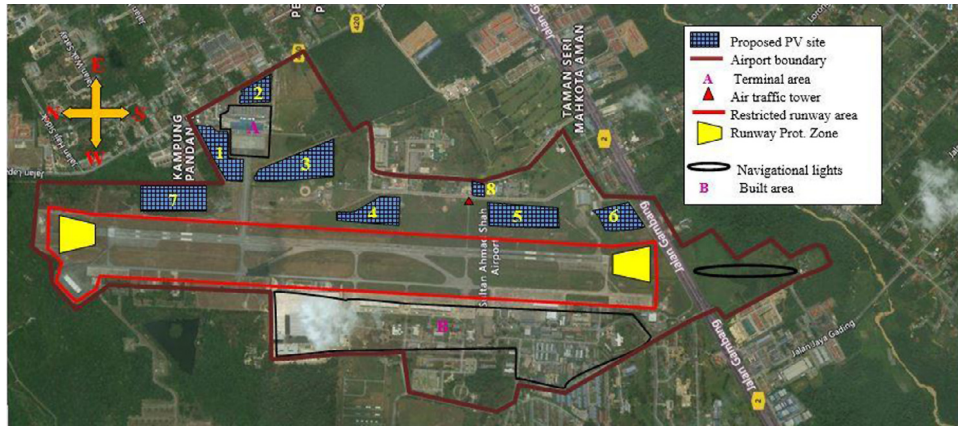


Fig. 1. Airport boundary and selected zones for proposed solar PV installation.

interval of time. This sun vector represents the axis of the conical sunbeam.

Step 8: The aperture of the conical sunbeam,  $\beta$  can be calculated using Eq. (10).

$$\beta = 2 \times \left( \frac{\theta_{\text{sun angle}}}{2} + 2 \times 3 \times \theta_{\text{slope error}} \right) \quad (10)$$

Step 5: This sunbeam is extrapolated from the observation point, OP towards the PV array. A conical section is considered at 1 m from the cone apex (OP). The axis of the cone is at right angles to the radius vectors of the conical section. The points that are lying on the edge of the conical beam as well as falling in the conical section are to be found. Since these points are orthogonal to the cone axis, the dot product of any two randomly chosen coordinates is zero. and are found using Eq. (11). About 30 points are established in this manner.

$$P_{ca} \cdot P_{ra} = 0 \quad (11)$$

where  $P_{ca}$  denotes vector on the cone axis and  $P_{ra}$  denotes the radial vector of the conical section.

Step 6: Conical edge vectors are found by subtracting the cone apex from the previously determined 30 co-planar points.

$$d = \frac{(p_0 - I_0) \cdot \vec{n}}{I \cdot \vec{n}} \quad (12)$$

where  $\vec{n}$  is the vector normal to the plane of PV array,  $I$  is one of the vectors between OP to the PV array,  $P_0$  is a point on the PV array,  $I_0$  is a point on the vector (the OP),  $d$  is the distance from the OP to the intersection point.

Step 7: If conical vectors intersect the PV array, these intersection points  $(x, y, z)$  are calculated using Eq. (13) (Wikipedia, 2019). The intersection of conical vectors with the PV array plane will result in an elliptical conical section.

$$(x, y, z) = dI + I_0 \quad (13)$$

Glare is present and strikes the OP if any of the vertices of PV array lie within the co-planar ellipse. It can be found using an optimized points-in-polygon algorithm (matplotlib, 2019).

The proposed zones of the solar PV array is located using the google map. The Observation Points (OP) considered for glare assessment in airports are the position of pilots during flight approach and air traffic controller in ATC tower. The location and height of the ATC tower are given. Generally, the height of ATC is more than 20 m (Shalya, 2009). A fixed-tilt solar plant consisting of PV panels with Anti Reflective coating (ARC) inclined at  $10^\circ$  tilt and oriented  $180^\circ$  from the north (true south) is considered.

Table 2  
Other input parameters are given for glare analysis.



Inputs	Definitions	Remarks
Ocular transmission coefficient	Accounts for the amount of radiation passing through the eye before reaching the retina.	Default value is 0.5
DNI (W/m <sup>2</sup> )	It refers to the amount of solar insolation in a straight line falling on the surface normal to sun rays for a particular duration (say 60 min).	Peak value of DNI is taken as 1000 W/m <sup>2</sup> .
Time interval (min)	Time duration of analysis	One minute is chosen
Eye focal length (m)	The distance between the nodal (point where rays intersect in the eye) and retina. This value helps to determine the size of the image that is projected on the retina for a given subtended angle of the glare source.	Typical focal length is 0.017 m
Pupil diameter (m)	Defines the diameter of the pupil of the observer receiving predicted glare. This size influences the amount of light entering the eye.	Typical value is 0.002 m for daylight and 0.008 m for night vision.
Subtended angle of the sun (mrad)	Denotes the angle subtended by the sun when seen from earth.	Average value of sun angle is 9.5 mrad or 0.5 degree
slope error (mrad)	Its value depends on the PV material	10 mrad by default

For those zones with the occurrence of glare, this prediction tool calculates the impact and duration of glare. The intensity of glare is shown either in green or yellow color. Table 3 provides the interpretation of the color code for glare impact. If glare is present from a particular zone, then that zone is not considered for the proposed PV system.

### 2.3. Solar photovoltaic power potential

The capacity of the solar plant can be calculated on the basis of available land area in the selected zone. The plant capacity varies with the selection of PV module technology and type of mounting system. This area calculation is carried out for cSi technology-based fixed-tilt solar PV plant. (Solar Power Plant Installations In Malaysia, 2018). The total area required for 1 MWp fixed-tilt solar power plant is taken as 3.38 acres in Malaysian condition. If  $A_{pv}$  is the area available for solar PV installation in a Zone, the installed

**Table 3**  
Summary of glare impact assessment.

Glare status	Color	Remarks	Is it adhering to FAA's glare policy
Absent	Nil	Free from glare hazard	Yes. Both ATC and flight path is free from glare
Present	Yellow 	Potential to cause an after-image	Adhered if yellow glare strikes only on the flight path. Also ATC is free from glare
	Green 	Low potential to cause an after-image	Green glare on ATC or flight path violates FAA's policy

**Table 4**  
General comparison of different PV technologies.

PV technology	Module efficiency (as per SolarGis manual)	Temperature coefficient of power (%/°C)	Global annual production (%)
Crystalline silicon (cSi)	13% to 20%	−0.44	} 20%–15%
Amorphous silicon (aSi)	5% to 8%	−0.21	
Cadmium Telluride (CdTe)	7% to 11%	−0.25	
Copper Indium Diselenide (CIS)	7% to 11%	−0.36	

capacity ( $P_c$ ) is estimated using Eq. (14).

$$P_c = \frac{A_{pv}}{3.38} \quad (14)$$

#### 2.4. Preliminary design of solar PV plant

It is assumed that the selected sites have a flat land area with minimal shadow effect. Fixed tilt PV systems have less weight, use less material and require less maintenance as compared to tracking systems. In this study, the ground-mounted fixed-tilt system is considered. This section describes the preliminary design procedures for MW scale solar PV systems. These design values are used as inputs to PV simulation software.

**Selection of PV module:** Commercially available PV technologies such as monocrystalline silicon (mono-cSi), multi (poly) crystalline silicon (multi-cSi), amorphous silicon (a-Si), Cadmium Telluride (CdTe) and Copper Indium Gallium Selenide (CIS) are suitable for solar PV system (Debbarmaa et al., 2017). The comparison of PV technologies in terms of efficiency, temperature coefficient and global annual production (as per SolarGis manual) is given in Table 4. The energy generation from each technology is estimated using SolarGis software. The solar PV module rating varies from a few watts to the range of hundred watts. For easy transportation, ease of installation and effective utilization of land area, PV modules with a power output rating of 300 W or above are normally chosen in MW scale solar PV installations.

**Selection of inverter:** The conversion of DC power generated from the PV panel to AC form occurs in an inverter. Central inverter configuration offers high reliability, simplicity in design and ease of installation. Three-phase inverters of 500 kW or more capacity is chosen for large scale solar PV systems. Highly efficient inverters (more than 95%) with total harmonic distortion less than 3% are chosen. It reduces power conversion losses and assures power quality.

**Selection of transformer:** In MW scale solar plant, the inverter output voltage is stepped up to higher voltage before feeding the energy to the utility grid. The transformer is selected in such a way that it has the least energy losses. So, transformers with an

efficiency of more than 95% are preferred. The voltage rating on the transformer's primary and secondary side must match with inverter rating and grid characteristics.

**Number of PV modules:** A certain number of modules are connected in a series to form a string and the number of PV modules in a string ( $N_s$ ) is calculated using Eq. (15). These high voltage (HV) rated strings are then connected parallelly to the inverter input terminals and form a string set (Shukla et al., 2016). The number of strings ( $S_p$ ) is estimated using Eq. (15a). The total number of PV modules,  $N_m$  required for the solar plant is found using Eq. (15b).

$$N_s = \left[ \frac{\text{avg}(V_1 + V_2)}{V_3} \right] \quad (15)$$

where  $V_1$  is the maximum value of the Maximum Power Point Tracking (MPPT) voltage of the inverter,  $V_2$  represents the minimum value of MPPT voltage of inverter and  $V_3$  denotes MPPT voltage of the PV module.

$$S_p = \left( \frac{P_c \text{ in watts}}{N_s \times P_{max}} \right) \quad (15a)$$

$P_c$  represents the proposed capacity of the PV plant and  $P_{max}$  denotes maximum power rating of the selected PV module

$$N_m = N_s \times S_p \quad (15b)$$

**Number of inverters:** The cumulative rating of the inverters ( $P_{inv}$ ) should be equal to the rated capacity for grid connected solar PV plants. It helps in efficient and safe operation. Most of the medium and large - scale solar PV plants have central inverter configuration. The number of inverters ( $N_{inv}$ ) needed for the proper operation of a solar PV system is found using Eq. (16).

$$N_{inv} = \left( \frac{N_s \times S_p \times P_{max}}{R_{DCtoAC} \times P_{inv}} \right) \quad (16)$$

where  $R_{DCtoAC}$  represents DC to AC ratio and is taken as 1 for the grid-connected solar PV system.

**Number of transformers:** The required number of transformers ( $N_{tr}$ ) can be found out using Eq. (17) where  $P_{tr}$  corresponds to the power rating.

$$N_{tr} = \left( \frac{N_s \times S_p \times P_{max}}{R_{DCtoAC} \times P_{tr}} \right) \quad (17)$$

**Tilt angle ( $\theta_t$ ):** The PV modules are to be fixed in such a way that maximum solar insolation strikes on its surface (Shukla et al., 2015). So, the inclination of the PV panel is taken as the latitude ( $l$ ) of the plant location. This is considered as the optimum value with respect to energy generation.

$$\theta_t = \text{latitude}(l) \quad (18)$$

**Orientation ( $\theta_{or}$ ):** The PV modules in the northern hemisphere are kept towards the south while that in the southern hemisphere is oriented towards the north. If the north direction is taken as the reference (zero degrees), then the PV system located in the northern hemisphere is oriented at an angle of 180 degrees from the reference.

$$\theta_{or} = 180^\circ \quad (19)$$

**Inter row distance (D):** The distance between two rows of PV array is called inter-row distance (D). It can be taken approximately as three times the height of the module from its lower end (h) (Kalita et al., 2019). The module height from the ground varies with module length ( $l_m$ ) and tilt angle ( $\theta_t$ ).

$$D = 3 \times h \quad (20)$$

where  $h = l_m \cdot \sin(\theta_t)$

### 2.5. Simulation using SolarGis and performance analysis

SolarGis is one of the best prediction tool available in the PV market. SolarGis has a geographic information system that is designed to meet the solar PV industry analytical requirements. This application combines solar resource data and meteorological data with a web-based application system (Shukla et al., 2017). It can be used in the planning, development, and operation of the solar energy system. It is a professional PV software used for pre-design assessment, yield assessment of photovoltaic power plants. The key features are easy selection of location, simulation using different PV technology, the variation of tilt angle and orientation angle. This software package includes applications such as iMaps (high resolution global interactive maps), Climate data, PV Planner, PV Spot. SolarGis–PV Planner’s trial version is used in the present research work. The flow of simulation in PVplanner is given in Fig. 2.

SolarGis software requires the user to provide data on the proposed solar PV system. At first, the location of the airport is given as location inputs because all the zones fall within the premises of the airport. The software takes data such as global radiation, diffuse radiation, ambient temperature and wind speed for the given location and uses it for the simulation. In the next step, the software allows the user to give technical parameters of the system. The estimated installed capacity is entered into the software considering the land availability and glare occurrence. The type of PV technology is chosen. The lifespan of good quality and well-maintained PV modules is more than 20 years (Sukumaran and Sudhakar, 2017a,b). A higher level of degradation may happen initially. i.e. the module degrades to 91% of its nominal power in the first year. A two-step power warranty (90% until 10 years and 80% until 20 years) has been given as the historical standard by the solar industry for the PV modules. The euro efficiency of the inverter is taken as 98%. The DC loss is assumed to be 5.5% and it includes self-shading of PV modules, external shading, soiling loss, loss due to mismatch of PV modules, DC cable, and interconnection loss. The losses in transformer and cables (AC losses) are considered as 1.5%. The availability of the grid is assumed as 99%. The mounting structure is chosen as free-standing which is easy to install with less chance for maintenance and glare occurrence. In order to obtain maximum energy yield, a tilt angle equal to the latitude of the location is generally considered. Though the latitude is 3°, a slightly higher tilt angle of 10° inclination is chosen to reduce the accumulation of dust. Since the location of Kuantan airport is in the Northern hemisphere, the solar modules are faced towards the south direction i.e. orientation angle of 180°. The value of the losses for the proposed plant is given in Table 5.

**Table 5**

The loss values considered for the proposed plant.

Plant loss particulars	Amount (%)	Remarks
Soiling loss	2%	Accumulation of dust occurs due to the low tilt angle
External shading	1%	Airport buildings may cast a shadow on PV array
Inter row shading	0%	Adequate spacing is provided between rows of PV array
Snow	0%	Tropical climate
Mismatch loss	0.5%	Lower value due to proper module selection
DC cable loss	2%	Power loss occurs due to central inverter topology
Inverter loss	2%	Highly efficient inverters are selected
AC cable loss	0.5%	Length of AC cable is more due to several transformer stations in the site
Transformer	1%	Transformers with less power losses are chosen
Unavailability	1%	Stable grid with a low occurrence of shutdown events
Total	10%	–

**PV performance assessment parameters:** The prediction of the performance from solar power is an important step in the process of execution of the solar project. Performance parameters are defined to evaluate the PV system with respect to energy production, solar resource, and system losses. Performance analysis provides a basis for the assessment of solar PV power plants and helps to develop practical recommendations for improving the operational performance of photovoltaic systems. The International Energy Agency (IEA) recommended the parameters for analyzing the performance of the grid-connected solar PV system. In the present study, the monthly variation of energy generation is obtained from PV software. and the performance parameters are estimated for the proposed solar system. Table 6 summarizes the performance indices used in the study.

**Energy generation:** It refers to the net electrical energy produced from the solar PV system. The energy generated from the solar system is represented mainly in three durations such as daily, monthly or yearly. In this study, the monthly energy generation is represented as  $E_{ac,m}$  and daily energy generation is shown as  $E_{ac,d}$ . The data logger measures the energy fed into the nearby electricity grid for a specific time interval (1 min or 5 min). The variation of energy output is a significant factor that determines the performance of the solar PV plant.

**Reference yield ( $Y_r$ ):** It can be estimated from the ratio of total in-plane irradiance ( $H_t$ ) to the reference irradiance ( $G_o$ ) on the PV array plane ( $1000 \text{ W/m}^2$ ). This yield refers to the number of hours per day at reference irradiance required to produce energy equivalent to the recorded incident solar irradiation.  $Y_r$  describes the solar radiation resource for the PV system which is a function of the location, PV array orientation, and weather variability.

**Array Yield ( $Y_a$ ):** It is defined as the ratio of monthly energy generation ( $E_{dc,m}$ ) at the input terminals of the inverter to the installed capacity of the solar PV power plant ( $P_c$ ). It is usually denoted in kWh/kWp. The  $E_{dc,m}$  value is the ratio between

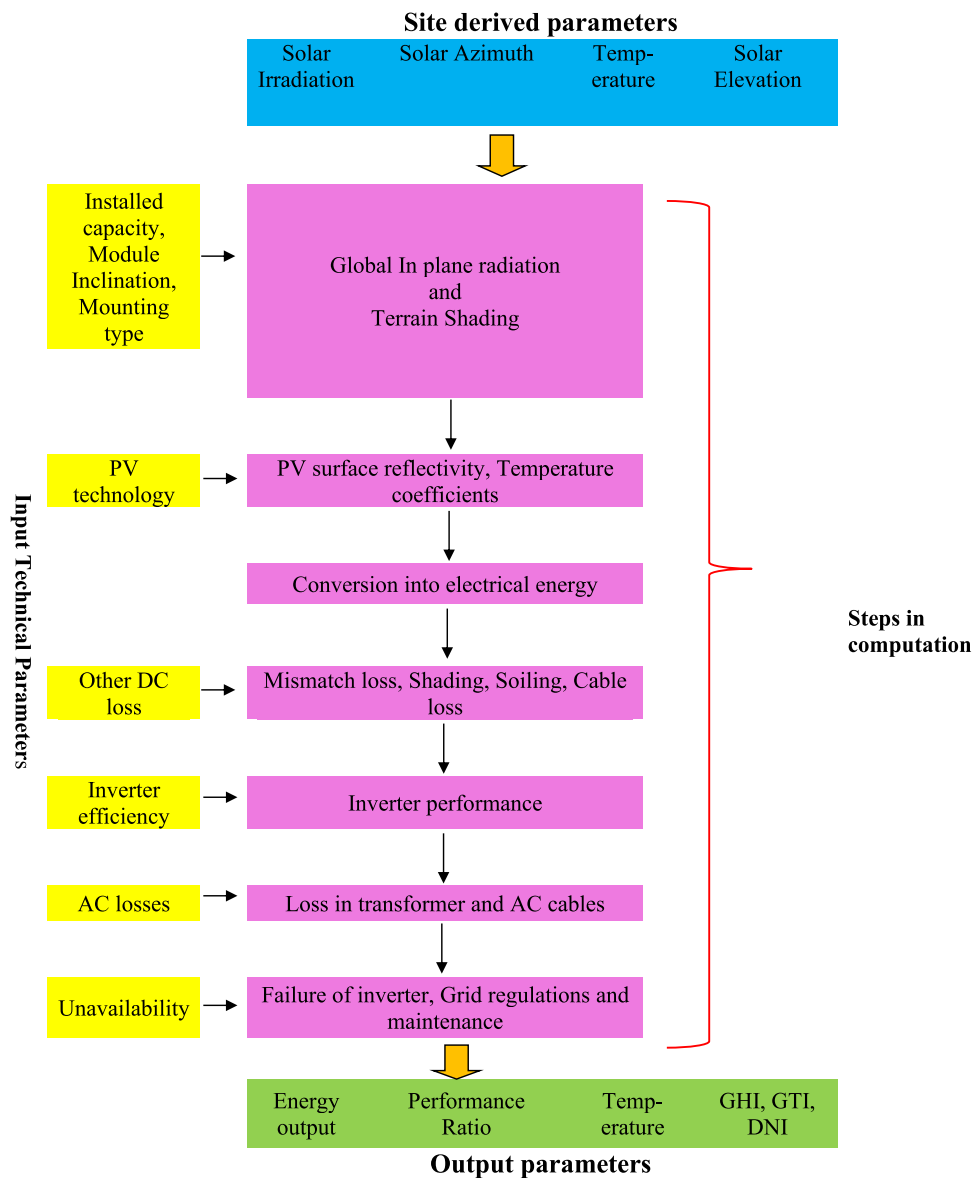


Fig. 2. Steps involved in SolarGis simulation of solar PV.

monthly AC energy generation ( $E_{ac,m}$ ) and the efficiency of the inverter ( $\eta_{inv}$ ).

**Final yield ( $Y_f$ ):** It is the ratio of monthly energy generated from the inverter's output terminal ( $E_{ac,m}$ ) and the installed capacity ( $P_c$ ) of the solar PV plant at Standard Test Conditions (STC) (Goura, 2015). The monthly final yield can also be described as the operational hours that a solar PV plant has to operate at its rated capacity so as to match the monthly energy generation. The final yield is denoted in kWh/kWp.

**Performance ratio (PR):** The ratio of final yield ( $Y_f$ ) and reference yield ( $Y_r$ ) gives the PR of the solar PV power plant. It quantifies the overall effect of losses that occurred during the operation of the solar plant (Sukumaran and Sudhakar, 2017a,b). The value of PR helps in detecting malfunction and failures in solar PV systems. It is expressed as a percentage or decimal. The PR value is independent of the installed capacity and location of the solar PV system. Hence it can be used to compare the performance of PV systems located anywhere in the world. The performance ratio acts as a comparable performance indicator among the grid-connected PV system. PR is a useful tool because it considers

the correctness of solar plant design and plant maintenance. The higher the value of performance ratio, the most desirable is the plant performance on-field.

**Capacity Utilization Factor (CUF):** The ratio between the electrical energy generation,  $E_{ac,m}$  and the maximum energy output (theoretical value) of the plant gives the monthly value of CUF. The theoretical energy generation is the product of installed capacity ( $P_c$ ) and the total number of hours in a month.  $N_d$  denotes the number of days in a month. A 1 MW PV power plant operating at 18% CUF generates energy equivalent to a power plant with an installed capacity of 0.18 MW and operating throughout the year (8760 h) without any interruption.

**Energy loss:** A portion of horizontal solar radiation is reduced by terrain shading and reflection from the PV module. The deviation of ambient temperature and the atmospheric conditions from STC reduces the power conversion in solar panels. In addition, power loss occurs in DC cables which connect solar panels and the inverters. This reduction is collectively termed as array capture loss. Energy is lost in inverters during power conversion. Also, energy loss occurs in transformers and AC cables. Also, the loss in



**Table 6**  
Summary of different relations of PV performance parameters.

Sl. No	Performance parameter	Formulae (monthly averaged values)
1	Energy generation	$E_{ac,m} = \sum_{d=1}^{d=N} E_{ac,d}$
2	Reference Yield	$Y_r = \frac{H_t}{G_o}$
3	Array Yield	$Y_a = \frac{E_{dc,m}}{P_c}$
4	Final Yield	$Y_f = \frac{E_{ac,m}}{P_c}$
5	Performance ratio	$PR = \frac{Y_f}{Y_r}$
6	Capacity Utilization Factor	$CUF = \frac{E_{ac,m}}{P_c \times 24 \times N_d}$
7	Capture Loss	$L_c = (Y_r - Y_a)$
8	System Loss	$L_s = (Y_a - Y_f)$
9	Plant efficiency	$\eta_p = \frac{E_{ac,m}}{A_m \times H_t}$

energy due to grid unavailability has to be considered. The losses in AC cables and inverters mainly account for the system loss.

- Array capture loss ( $L_c$ ) is the difference between reference yield ( $Y_r$ ) and array yield ( $Y_a$ ).
- System loss ( $L_s$ ) is the difference in values of array yield ( $Y_a$ ) and final yield ( $Y_f$ ).

Plant Efficiency ( $\eta_p$ ): It is the ratio of AC energy generation ( $E_{ac,m}$ ) to the product of monthly solar irradiation ( $H_t$ ) and PV module area ( $A_m$ ). The PV module efficiency at STC is always higher than the plant efficiency.

The steps involved in the present study is given in Fig. 3.

### 3. Results and discussions

The solar PV power plant is proposed for different locations of Kuantan airport. The glare assessment is carried out for each site. The simulation is carried out for a hypothetical 20 MW solar power plant in the aerodrome and its performance is analyzed based on parameters such as performance ratio, final yield, capacity factor, etc.

#### 3.1. Solar resource assessment

The monthly variations of solar irradiation and air temperature are presented. The horizontal irradiation is 123.6 kWh/m<sup>2</sup> in January and reaches the highest value of 162.4 kWh/m<sup>2</sup> in March. In the consecutive months, solar radiation decreases to reach 144.9 kWh/m<sup>2</sup> in June. A second peak is observed in the month of September which is again followed by a rapid decrease to reach the lowest point of 111.4 kWh/m<sup>2</sup>. The historical values of solar irradiation and temperature are obtained from SolarGis and shown in Fig. 4. The solar energy generation depends heavily on solar insolation received at the site. Since solar radiation has reasonable variation throughout the year, the energy generation from the solar plant also fluctuates throughout the year. The ambient temperature at the proposed site varies between 24.7 °C and 26.9 °C. The temperature of the PV module mainly depends on the ambient temperature. As the module temperature increases, the energy output of the PV module reduces. The average air temperature in the plant site is around 26 °C and is close to the temperature value at Standard Test Conditions. The plant site receives an ample amount of solar radiation around the year, and the ambient temperature stays without much variation. As per

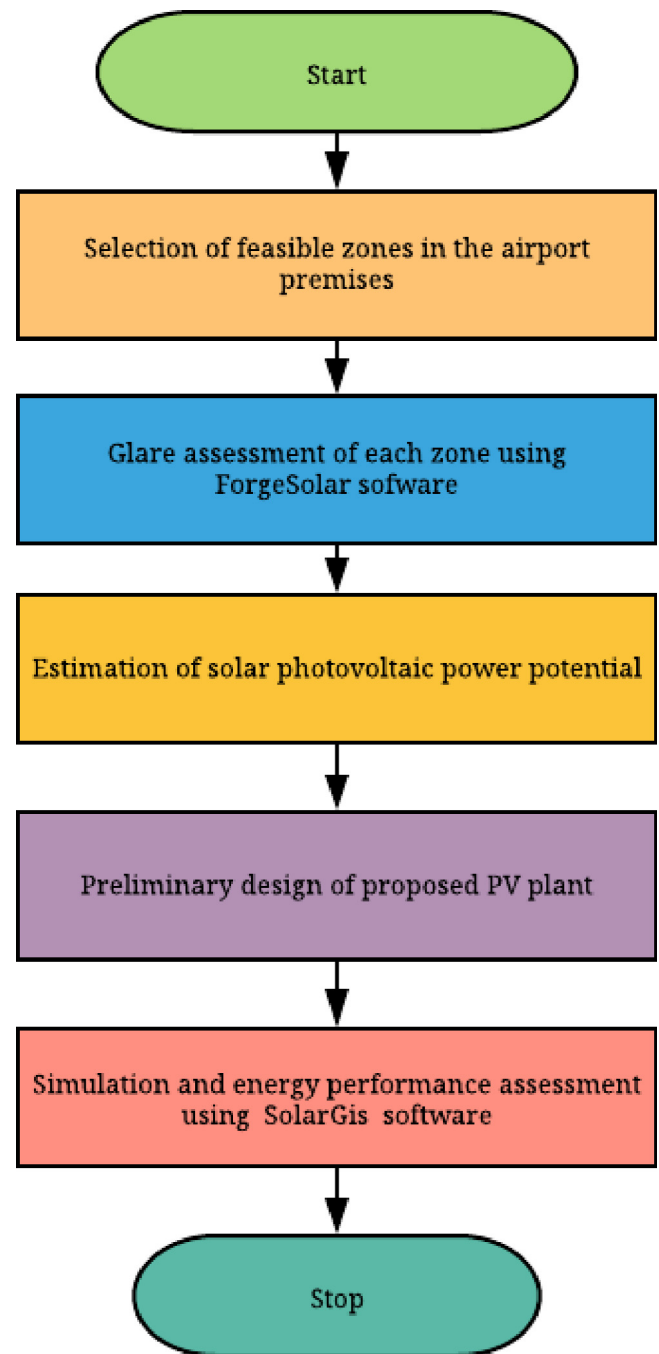


Fig. 3. Flowchart for the proposed methodology.

the wind data from NASA's MERRA-2 satellite, the average wind speed in the Kuantan region has significant variation throughout the year. The windier part of the year begins from the middle of November and ends in the first week of March with an average wind speed of 3.13 m/s. The remaining part of the year is calm. The lowest value of the average wind speed is 1.92 m/s (NASA MERRA 2, 2020).

From the favorable weather information like irradiation, ambient temperature, and wind speed, it can be said that the climatic conditions in Kuantan are suitable for the proposed solar PV power plant.



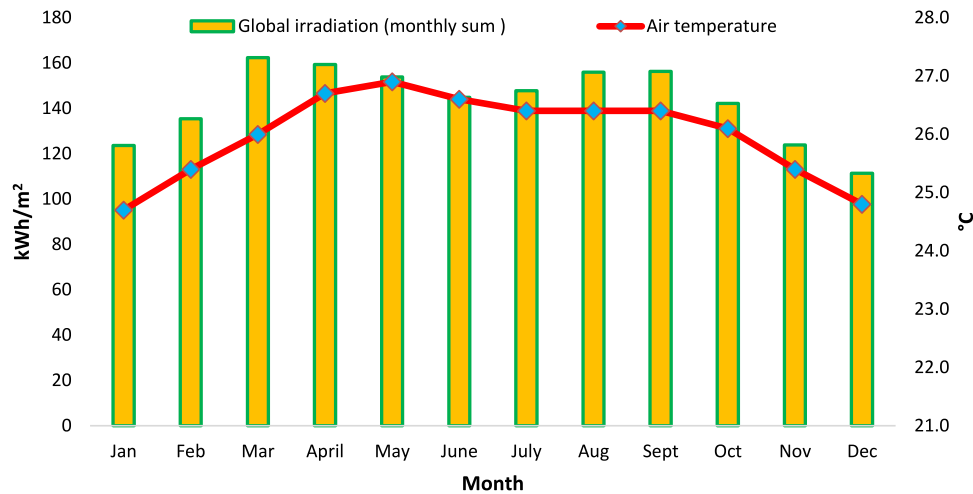


Fig. 4. Variation of solar irradiation and air temperature.

### 3.2. Glare assessment

Glare assessment is carried out in the eight selected zones using ForgeSolar software to check its compatibility as per the glare policy of the Federal Aviation Administration (FAA). The glare is absent from all the zones except zone 8. The important results of glare analysis are summarized in Table 7.

The solar PV module installation in Zone 8 will affect the visibility of air traffic controllers from ATC tower since glare occurs for 4552 min over the entire year. It is predicted that yellow glare (the potential to cause temporary after-image) occurs for 4552 min and green glare (low potential to cause temporary after-image) does not occur at all. The predicted glare is expected to strike in the morning and last for about 30 to 40 min, starting from the middle of April to the end of September as shown in Fig. 5. At the same time, the glare strike on the Flight Path (FP) is nil which can be attributed to the distance between Zone 8 and the observer point (pilot's eye). Out of the eight sites, Zone 8 is not selected as it violates the glare policy of the FAA. The glare impact results for Zone 8 are shown in Table 8.

### 3.3. Solar photovoltaic power potential

Seven zones are selected for the proposed solar PV system at Kuantan airport. The cumulative capacity of these zones is 20 MW (Fig. 6). The solar power potential for Zone 1, Zone 2, Zone 3, Zone 4, Zone 5, Zone 6, Zone 7 is 2 MW, 1.5 MW, 4 MW, 2.5 MW, 3 MW, 2 MW, 5 MW respectively. Zone 7 has a larger area among other zones and hence has the highest solar power potential. Zone 2 can produce only 1.50 MW of power as it covers less area.

### 3.4. Solar PV plant design

The proposed 20 MW grid-connected solar plant covers an area of 66.67 acres. The main components of a utility-scale solar power plant are arrays of solar PV modules, inverters or power conditioning units (PCU), transformers etc.

**Selected PV technology:** Four commercial PV technologies are compared in terms of predicted energy generation values obtained from SolarGis software. The respective annual energy production is 1315.2 MWh (cSi), 1455.2 MWh (CdTe), 1442.4 MWh (aSi), 1332.7 MWh (CIS). As compared to crystalline silicon PV (cSi) technology, the percentage increase in energy output is 1.11% (CdTe), 1.09% (aSi) and 0.98% (CIS). It was observed that thin-film technologies have slightly higher energy generation

than crystalline silicon PV modules (see Fig. 7). The cSi PV modules have the lion's share of the solar PV market. Most of the airport installations have cSi PV technology based solar installation (Mpholo et al., 2014; Sukumaran and Sudhakar, 2017a,b). Monocrystalline silicon PV modules have higher efficiency than polycrystalline PV modules. So monocrystalline solar modules are a good fit for the proposed solar PV plant. The PV modules of 350-w power rating (LR4-60HPH-350M) manufactured by the solar manufacturer in Malaysia is chosen for the study. The electrical properties of the PV module selected for the proposed power plant are given in Table 9. Solar modules manufactured in Malaysia are chosen because of their easy availability and reduced transportation cost.

**PV array:** The proposed solar PV plant consists of 57,143 solar PV modules. The number of modules in a string is 20. The number of strings in the PV array is 2857.

**Inverter:** Central inverters of 500 kWp nominal ratings are chosen. The energy generated from the site is converted to AC output using the inverter. The number of inverters needed for the proposed solar PV plant is 40. The electrical properties of the inverter are given in Table 10.

**Transformers:** Each transformer has a power rating of 1 MVA. The number of transformers required is 20. In certain cases, a single transformer receives power from more than one zone. The energy generated is fed to the existing grid of the airport's electrical facility.

**Plant layout:** The PV modules are mounted on fixed structures at an inclination angle of 10 degrees, facing south. The orientation angle is 180°. The tilt angle is kept at 10 degrees to reduce dust accumulation and to aid self-cleaning. The inter-row distance is estimated as 0.924 m. The gap between the two sections is taken as 2 m. This helps during rescue operations such as accidental incursion into PV array by aircraft, fire hazard, etc (Mostafa and Zobia, 2016). The plant is assumed to be divided into a number of sections of the PV array and such arrangement is advantageous during plant breakdown. For a simpler layout, it is taken that a single section consists of 32 rows of PV modules and each row contains 20 numbers of solar modules. Apart from sitting in PV modules, space is needed for inverter rooms, fencing, remote office etc. The general layout for the solar PV system is given in Fig. 8.

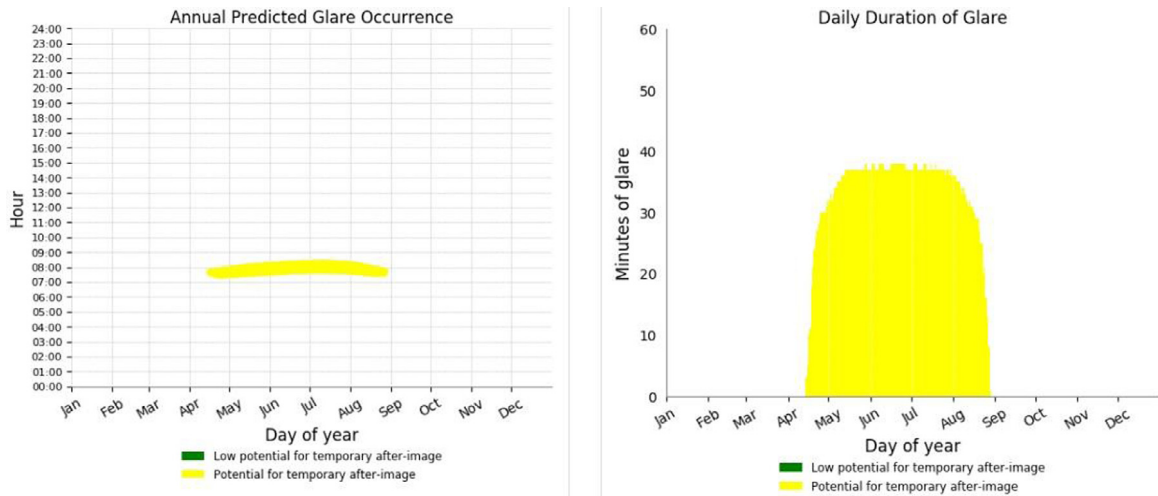


Fig. 5. Annual predicted glare occurrence and its daily duration for Zone 8.

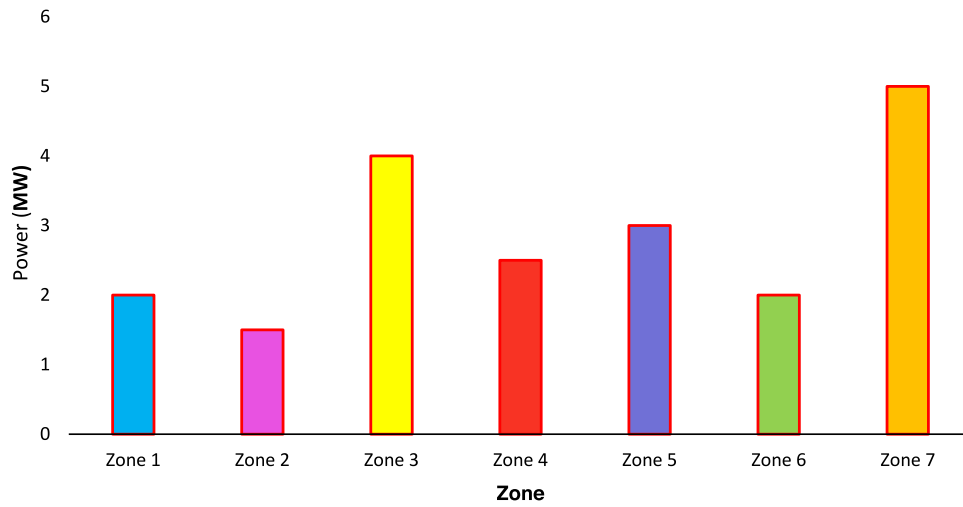


Fig. 6. Solar power potential of the selected zones in Kuantan airport.

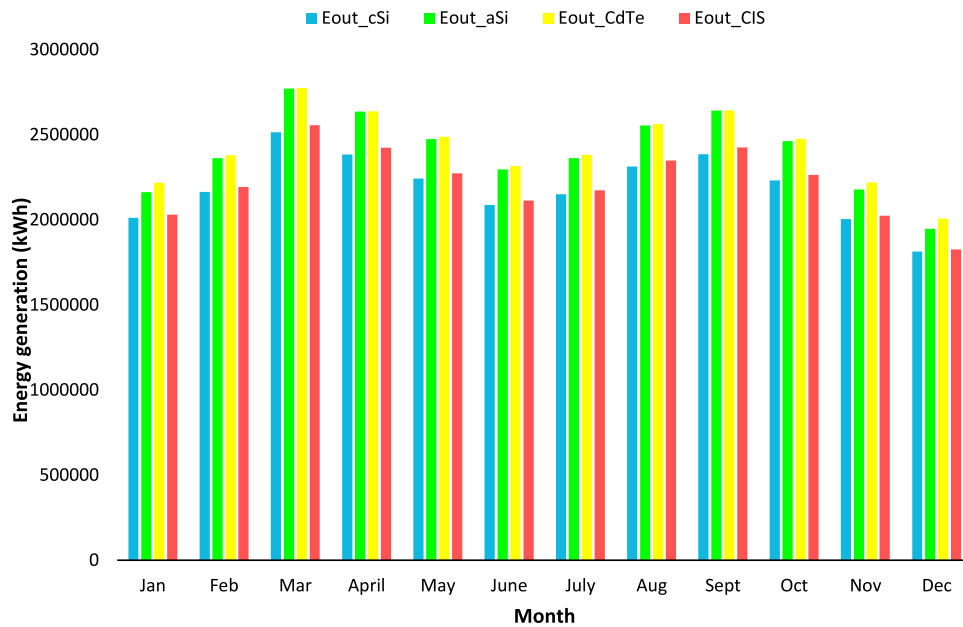
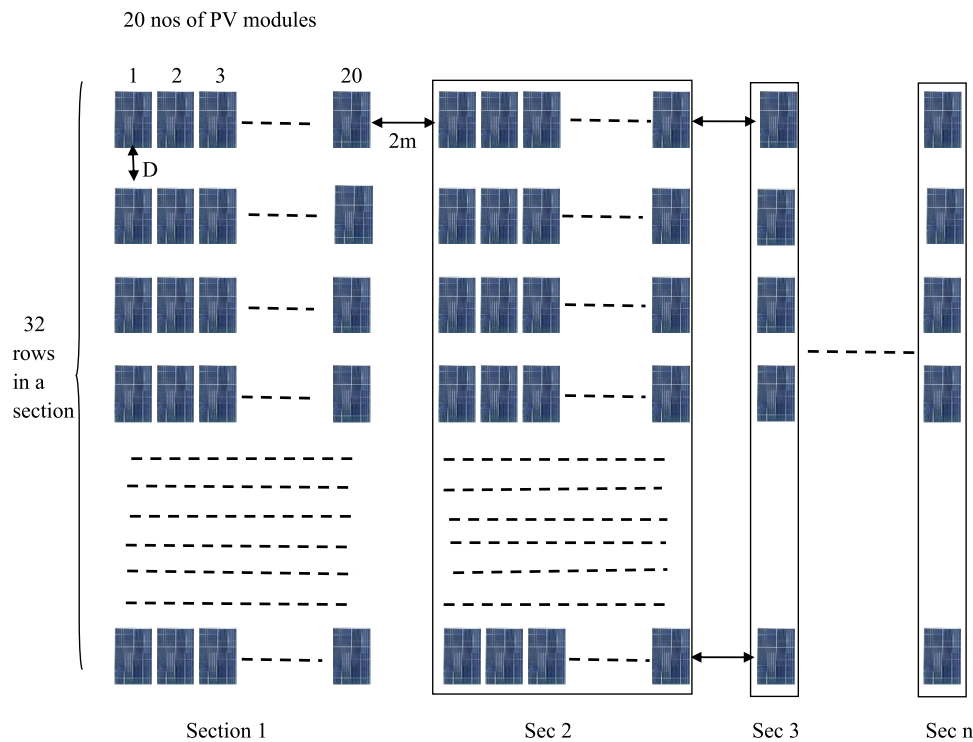


Fig. 7. Monthly variation of energy generation at the airport site.

**Table 7**  
Solar potential and glare impact of selected zones in Kuantan airport.

Sl. No:	Site/Zone	Solar power potential (MW)	Glare occurrence		Is the site compactible with FAA's glare policy
			Green glare (mins)	Yellow glare (mins)	
1	Zone 1	2.0	No	No	✓
2	Zone 2	1.5	No	No	✓
3	Zone 3	4.0	No	No	✓
4	Zone 4	2.5	No	No	✓
5	Zone 5	3.0	No	No	✓
6	Zone 6	2.0	No	No	✓
7	Zone 7	5.0	No	No	✓
8	Zone 8	0.71	No	Yes	×
Total solar potential with glare				20.71 MW	
Total solar potential without glare				20.0 MW	



**Fig. 8.** Pictorial representation of the arrangement of solar PV modules.

**Table 8**  
Results of glare analysis on the Zone 8.

Zone with glare occurrence	Receptor	Green glare (min)	Yellow glare (min)
Zone 8	Flight path	0	0
	ATC tower	0	4552

**3.5. Performance analysis**

The proposed 20 MW solar power plant in airport premises generates 26,304 MWh annually. The peak power generation is observed in the months of March (2514 MWh), September (2386 MWh) and April (2384 MWh). This can be correlated with the high values of solar insolation available in these months. The lowest power output is observed in the month of December which in turn reduces the CUF. The annual energy production from the proposed solar PV plant is 168 times the energy requirement of the passenger terminal (Fig. 9). The electrical energy demand of terminal building is 155.89 MWh annually. It is also observed that supply from solar PV plant matches the energy load profile.

**Table 9**  
Electrical properties of the selected PV module.

Electrical parameters	Values (STC)	Value (NOCT)
Maximum power ( $P_{max}$ )	350 W	259.30 W
Open circuit voltage ( $V_{oc}$ )	40.5 V	37.8 V
Short circuit current ( $I_{sc}$ )	11.02 A	8.90 A
Voltage at max power	33.30 V	30.80 V
Current at max power	10.52 A	8.44 A
Module efficiency	18.7%	
Temperature coefficient of $I_{sc}$	+0.057%/°C	
Temperature coefficient of $V_{oc}$	-0.286%/°C	
Temperature coefficient of $P_{max}$	-0.370%/°C	
Power output tolerance	up to 5 W	
$V_{oc}$ and $I_{sc}$ tolerance	±3%	
Maximum System Voltage (DC)	1500 V	

Kuantan being a rural airport, the energy demand is not huge, and it spreads across vast areas. Hence the energy consumption of rural airports can be met easily from solar power generation.

**Variation of yield parameters:** It was observed that the maximum value for both the array and final yield falls in March.

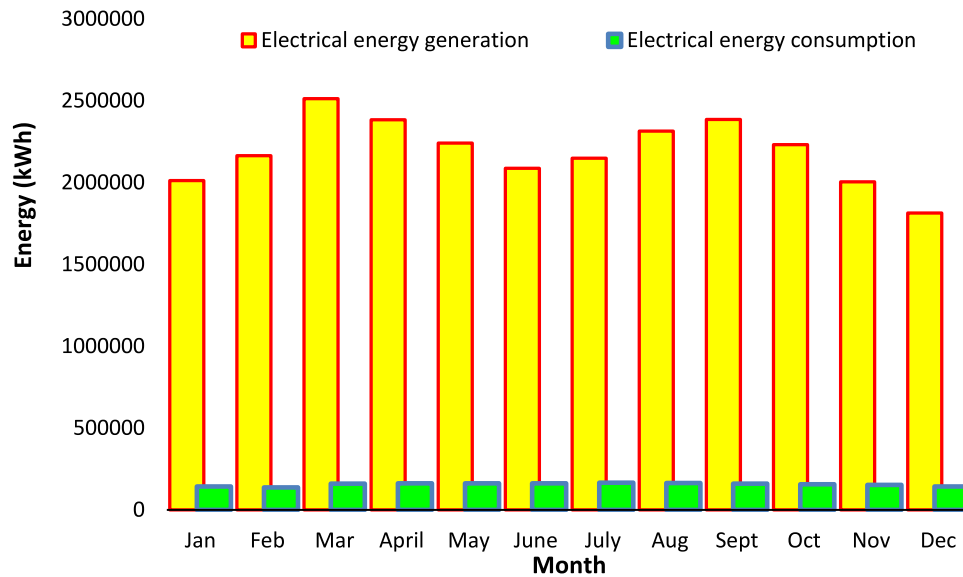


Fig. 9. Monthly variation of electricity consumption in terminal building and energy production in solar plant.

Table 10

Electrical specifications of inverter.

Parameters	Values
<b>DC side</b>	
Max. voltage	1000 V
Max. current	1250 A
Max. power	560 kW
MPPT voltage range at 25 °C	449 V to 850 V
<b>AC side</b>	
Nominal voltage	270 V
Max. Current	1176 A
Max. Efficiency (euro)	98.4%

The reference yield depends on the daily solar radiance received in the PV array. As the solar insolation increases, the reference yield also rises. Fig. 10 shows the monthly variation of reference yield, array yield and final yield. The monthly average final yield varies with a minimum value of 90.70 MWh/MWp-month in December to a maximum of 125.70 MWh/MWp-month in March. This variation can be attributed to the monthly average horizontal irradiation which is minimum for the month of December and maximum in the month of March. The value of the final yield is 100.60 MWh/MWp-month in January followed by a gradual rise in the value, to reach the peak in March. The final yield decreases gradually during the period from March to June and then rises steadily to reach the second peak in September (119.30 MWh/MWp-month). The lowest energy yield occurs in December. The reference and final yield have similar variation in the observed period since both depend on the value of in-plane solar radiation. The difference between the reference and final yield corresponds to the energy loss in the solar plant. The value of energy loss indicates a reduction in energy output as compared to that at STC conditions.

#### Variation of Performance Ratio and Capacity Utilization Factor:

The average value of PR is 76.88% indicating an acceptable operation. The variation of PR and Capacity Utilization Factor CUF over a specific period is shown in Fig. 11. It is observed that the performance ratio did not follow the change in solar irradiation. The highest performance ratio of 79.56% is observed in the month of December with low solar irradiation (111.4 kWh/m<sup>2</sup>) and minimum PR (73.62%) is observed in the month of June (144.9 kWh/m<sup>2</sup>). The energy loss from solar PV plants

increased during the months of higher solar irradiation which in turn reduced the value of PR. The value of CUF varies between 12.6% and 17.46%. The variation in CUF can be attributed to the value of the final yield which depends on the amount of electrical energy generation. The CUF of the proposed 20 MW has two peak sections. The first peak occurs between January to June, of which the peak value occurs in March (17.46%). From June onwards, the CUF value gradually increases and reaches a second peak in the month of September (16.57%), followed by a reduction in CUF value to dip to the lowest (12.6%) in December. The monthly averaged value of CUF for this proposed solar plant is 15.22%. This value fits into the range of CUF for solar PV systems in South East Asian countries ([Solar Power Plant Installations In Malaysia, 2018](#)). The performance ratio of the PV system can be improved by reducing the module temperature. The cooling of the PV surface can be done by the circulation of water or air and by using phase-change material. The spraying of water on the PV array showed a reduction in the module temperature. However, water is wasted in this process. The immersion of PV modules in the water at an exact depth improves the conversion efficiency and reduces water loss. But the implementation of this technique for large scale solar systems is difficult. The use of phase change material improves the performance of the PV system. The absorbing abilities of the material vary in hot and cold weather. The cooling of PV by air circulation is not effective when compared to water. An additional techno-economic analysis is needed to select the suitable cooling strategies for the proposed solar PV system.

The performance of the proposed solar plant is compared with solar PV installations in the airport and shown in Table 11.

**Energy losses:** The monthly variation of loss parameters (capture and system) and plant efficiency is given in Fig. 12. The energy loss in solar plant increases from January (25.9 MWh/MWp), reaches a peak value in March (37.0 MWh/MWp) and remains almost constant till September. This variation can be attributed to climatic conditions mainly the change in solar irradiation and ambient temperature at the site. The system loss (gray-blue color) is small when compared to capture loss (dark pink). As the energy loss increases, the energy output from the solar plant reduces ([Sukumaran and Sudhakar, 2018](#)). The average value of energy efficiency for the proposed solar PV plant is 11.54%. The efficiency curve resembles a quadratic polynomial an inverse relationship is observed between the plant losses and overall efficiency as seen in Fig. 12.



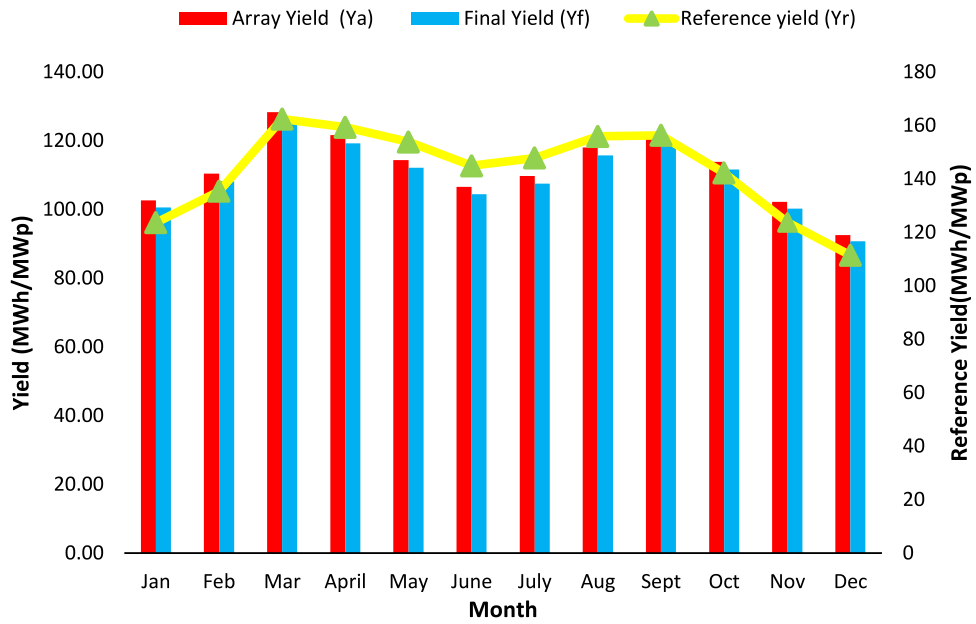


Fig. 10. Monthly variation of reference yield, array and final yield.

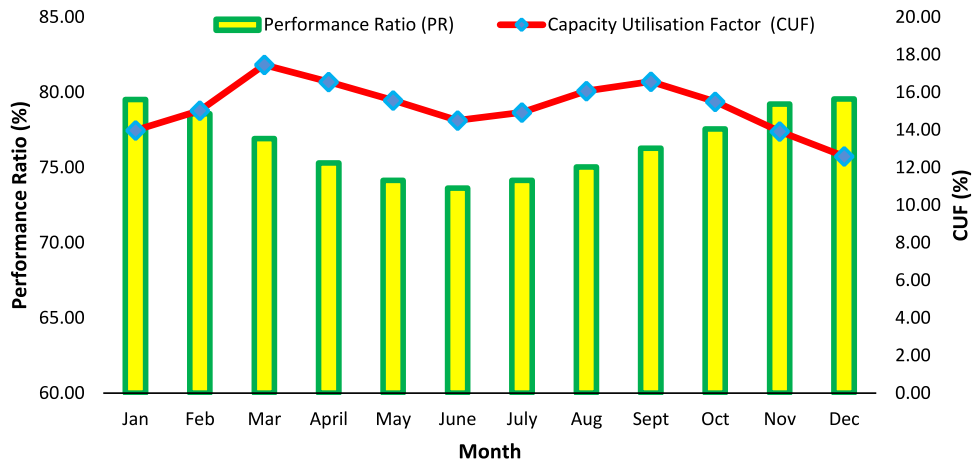


Fig. 11. Monthly variation of capacity utilization factor and performance ratio.

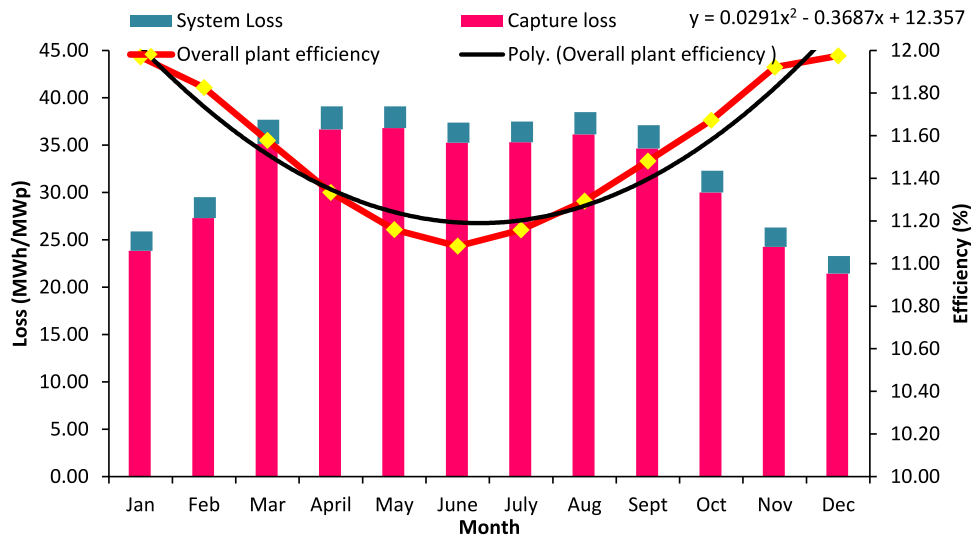


Fig. 12. Variation of capture, system losses, and plant efficiency.

**Table 11**  
Comparison of performance parameters of airport-based solar installations.

Airport Name, Country	PV technology	Installed capacity (kW)	Is glare analysis reported	Annual energy yield (kWh/kWp)	Avg. PR (%)	Avg. CUF (%)	Reference
Cochin airport, India	Poly-cSi	12 000	No	1984.10	86.56	20.12	Sukumaran and Sudhakar (2017a)
Moshoeshoe I airport, Lesotho	Poly-cSi	281	No	1501.20	70.00	–	Mpholo et al. (2014)
Kamuzu airport, Malawi	HiT <sup>a</sup>	830	No	1551.25	79.50	17.7	Banda et al. (2019)
Kuantan airport, Malaysia	Mono-cSi	20 000	Yes	1315.20	76.88	15.22	Present work

<sup>a</sup>HiT: Heterojunction with Intrinsic Thin layer.

**Table 12**  
Losses occurred in energy conversion of the proposed solar PV plant.

Sl. No:		PV output (MWh/MWp)	Energy lost in each step (MWh/MWp)
1	Total solar in-plane irradiation (input)	1708	
2	Effect of terrain shading	1707	1.0
3	Loss from solar reflections	1650	57.0
4	DC Conversion in PV modules	1456	194.0
5	Other DC losses	1376	80.0
6	Inverter loss	1349	27.0
7	Transformer and AC cable loss	1329	20.0
8	Loss due to grid unavailability	1315	14.0
Total energy lost			393

It was observed that around 400 MWh of energy is lost per MWp during the entire power conversion in the proposed solar PV plant. Among the energy conversion steps given in Table 12, the energy loss is highest during the generation of DC electricity, and it accounts for 11.70% of the total energy lost. This is followed by a loss of energy in the DC section, collectively termed as other DC losses, which include combined effect due to PV module mismatch, heat losses in power cables, interconnections and losses due to dirt, snow, icing, soiling, etc. Around 57 MWh/MWp of energy is lost due to reflection from the surface of the PV panel, which is typically made of glass. The predicted global in-plane irradiation by the software is 1708 MWh/MWp. Because of the satisfactory design of the solar plant, the losses in the inverter, transformer, AC cable and due to grid unavailability are relatively low. The euro efficiency of the chosen inverter is 98%. The transformer and AC cable loss are very low, and it is 20 MWh/MWp. The grid unavailability caused by the maintenance or failure in the electric utility is only 1% of the total utilization time which in turn restricts the energy loss value at 14 MWh/MWp. A portion of the global irradiation falling on the PV panel surface is reduced due to the obstruction of the terrain horizon.

#### 4. Conclusions

In this paper, different locations within an airport are chosen for the solar plant. The glare assessment is carried out for each zone. The performance of the proposed solar plant on the premise of Kuantan airport, Malaysia is estimated and the following conclusions are made.

- The mandatory free space around the runway can be effectively allocated for the solar power plant. Out of the eight selected zones, the glare impact is observed from Zone 8 only. It was predicted that yellow glare occurs for 4552 min on ATC during the morning time. This can be attributed to

the close radial distance between the observation point and the proposed PV array.

- The cumulative solar photovoltaic power potential of seven zones is 20 MW. Zone 7 has the highest solar potential and Zone 2 has the lowest potential. Solar power potential depends on the area of the selected zone.
- The proposed solar PV plant consists of 57,143 crystalline silicon PV modules. The number of modules in a string is 20. The number of strings in the entire PV plant is 2857. The proposed PV plant needs 40 numbers of central inverters and 20 numbers of transformers.
- The proposed solar PV power plant is expected to generate 26,304 MWh annually. The annual energy production from the proposed solar PV plant surpasses the energy requirement of the airport's terminal building (168 times). The electricity energy requirement of Kuantan airport can be made self-sufficient through solar PV installations.
- It was observed that the monthly average final yield varies from a maximum value of 125.70 MWh/MWp-month in March to a minimum of 90.70 MWh/MWp-month in December. The monthly averaged values of performance ratio and capacity utilization factor are 76.88% and 15.22% respectively. The overall efficiency of the solar plant is 11.54%. The energy lost during power conversion is 393 MWh/MWp. It can be concluded that the proposed solar plant performs sufficiently well.
- Solar-powered airports showcase a promising path towards sustainable aviation scenario. This research study on the performance of solar PV plants in Malaysian airports will be useful to researchers, energy policymakers and other professionals.

#### Declaration of competing interest

The authors declare that they have no known competing financial interests or personal relationships that could have appeared to influence the work reported in this paper.

#### CRedit authorship contribution statement

**S. Sreenath:** Writing - original draft, Software, Investigation, Data curation. **K. Sudhakar:** Conceptualization, Supervision, Investigation, Methodology, Writing - review & editing. **Yusop A.F.:** Supervision, Writing - review & editing. **E. Solomin:** Writing - review & editing. **I.M. Kirpichnikova:** Writing - review & editing.

#### Acknowledgment

This study was supported by Universiti Malaysia Pahang (UMP) through Doctoral Research Scheme (DRS) and Internal grant (RDU 1803100). The authors are grateful to Mr. Norsiam Bin Noordin (Head of Engineering, Kuantan airport), ForgeSolar and SolarGis software.

## References

- Alba, S.O., Manana, M., 2016. Energy research in airports?: A review. pp. 1–19, <http://dx.doi.org/10.3390/en9050349>.
- Anurag, A., Zhang, J., Gwamuri, J., 2017. General design procedures for airport-based solar photovoltaic systems. pp. 1–19, <http://dx.doi.org/10.3390/en10081194>.
- Banda, M.H., Nyeinga, K., Okello, D., 2019. Performance evaluation of 830 kw grid-connected photovoltaic power plant at Kamuzu International Airport-Malawi. *Energy Sustain. Dev.* 51, 50–55. <http://dx.doi.org/10.1016/j.esd.2019.05.005>.
- Barrett, S., Devita, P., Ho, C., Miller, B., 2014. Energy technologies compatibility with airports and airspace: Guidance for aviation and energy planners. *Airport Manage.* 8 (4), 1750–1946.
- Chikh, M., Mahrane, A., Bouachri, F., 2011. PVSST 1.0 sizing and simulation tool for PV systems, 6, 75–84. <http://dx.doi.org/10.1016/j.egypro.2011.05.009>.
- Choi, Y., Rayl, J., Tammineedi, C., Brownson, J.R.S., 2011. PV Analyst: Coupling arcgis with TRNSYS to assess distributed photovoltaic potential in urban areas. *Sol. Energy* 85 (11), 2924–2939. <http://dx.doi.org/10.1016/j.solener.2011.08.034>.
- Debbarmaa, M., Sudhakar, K., Baredar, P., 2017. Thermal modeling, exergy analysis, performance of BIPV and BIPVT: A review. *Renew. Sustain. Energy Rev.* 73, 1276–1288.
- Goura, R., 2015. Analyzing the on-field performance of a 1-megawatt-grid-tied PV system in South India. 34(1), 1–9.
- Gurupriya, T., Rix, A.J., 2017. Pv simulation software comparisons: Pvsyst, nrel sam and pvlb, (january). Retrieved from <https://www.researchgate.net/publication/313249367>.
- Ho, C.K., 2013. Relieving a glaring problem in solar today. *Amer. Solar Energy Soc.* 28–31.
- Kalita, P., Das, S., Das, D., Borgohain, P., Dewan, A., Banik, R.K., 2019. Feasibility study of installation of MW level grid connected solar photovoltaic power plant for northeastern region of India. *Sadhana* 44 (9), <http://dx.doi.org/10.1007/s12046-019-1192-z>.
- Kilkis, S., Kilkis, S., 2016. Benchmarking airports based on a sustainability ranking index. *J. Cleaner Prod.* 130, 248–259.
- Kumar, B.S., Sudhakar, K., 2015. Performance evaluation of 10 MW grid connected solar photovoltaic power plant in India. *Energy Rep.* 1, 184–192. <http://dx.doi.org/10.1016/j.egy.2015.10.001>.
- Lalwani, Mahendra Kothari, D.P., Singh, M., 2010. Investigation of solar photovoltaic simulation softwares. *Int. J. Appl. Eng. Res.* 1 (3), 585–601.
- Massachusetts Institute of Technology, 2019. Airline industry overview. from [http://web.mit.edu/airlines/analysis/analysis\\_airline\\_industry.html](http://web.mit.edu/airlines/analysis/analysis_airline_industry.html) (Retrieved December 26, 2019).
- matplotlib, 2019. Path. from [https://matplotlib.org/1.2.1/api/path\\_api.html#matplotlib.path.Path.contains\\_points](https://matplotlib.org/1.2.1/api/path_api.html#matplotlib.path.Path.contains_points) (Retrieved June 11, 2020).
- Mostafa, M.F.A., Zobaa, A.F., 2016. Risk assessment and possible mitigation solutions for using solar photovoltaic at airports.
- Mpholo, M., Nchaba, T., Monese, M., 2014. Yield and performance analysis of the first grid-connected solar farm at moshoeshoe i international airport, lesotho. *Renew. Energy* 81 (2015), 845–852. <http://dx.doi.org/10.1016/j.renene.2015.04.001>.
- NASA MERRA 2, 2020. Modern-era retrospective analysis. from <https://gmao.gsfc.nasa.gov/reanalysis/MERRA-2/> (Retrieved January 14, 2020).
- Padmavathi, K., Daniel, S.A., 2013. Performance analysis of a 3 MWp grid connected solar photovoltaic power plant in India. *Energy Sustain. Dev.* 17 (6), 615–625. <http://dx.doi.org/10.1016/j.esd.2013.09.002>.
- Personal Communication, 2020. Head of engineering, Kuantan airport.
- Rowlings, A., 2016. Sustainable energy options for the future airport metropolis.
- Rubeis, Tullio De Nardi, I., Paoletti, Di, Domenica, Ambrosini, Antonella, Dario Poli, R., Farra, S., 2016. Multi-year consumption analysis and innovative energy perspectives?: The case study of Leonardo da Vinci International Airport of Rome. *Energy Convers. Manage.* 128, 261–272. <http://dx.doi.org/10.1016/j.enconman.2016.09.076>.
- Shalya, C., 2009. Building blocks removed around airport areas. Retrieved February 17, 2017, from [http://timesofindia.indiatimes.com/articleshow/4817936.cms?utm\\_source=contentofinterest&utm\\_medium=text&utm\\_campaign=cppsthttps://timesofindia.indiatimes.com/city/mumbai/Building-blocks-removed-around-airport](http://timesofindia.indiatimes.com/articleshow/4817936.cms?utm_source=contentofinterest&utm_medium=text&utm_campaign=cppsthttps://timesofindia.indiatimes.com/city/mumbai/Building-blocks-removed-around-airport).
- Shukla, A.K., Sudhakar, K., Baredar, P., 2016. Design, simulation and economic analysis of standalone roof top solar PV system in India. *Sol. Energy* 136 (July), 437–449. <http://dx.doi.org/10.1016/j.solener.2016.07.009>.
- Shukla, A.K., Sudhakar, K., Mamat, R., 2017. Experimental exergy analysis of water-cooled PV module. *Int. J. Exergy* 3.
- Shukla, K.N., Sudhakar, K., Rangnekar, S., 2015. Estimation and validation of solar radiation incident on horizontal and tilted surface at Bhopal, Madhya Pradesh. *Am. Eur. J. Agric. Environ. Sci.* 1, 129–139.
- Siraki, A.G., Pillay, P., 2010. Comparison of PV System Design Software Packages for Urban Applications. *IEEE*, p. 12, Retrieved from <http://www.indiaenergycongress.in/montreal/library/pdf/285.pdf>.
- Solar Power Plant Installations In Malaysia. 2018. Retrieved December 16, 2018, from <http://aer.global/topic-13-solar-power-plant-installations-in-malaysia/>.
- Somcharoenwattanaa, W., Menkea, C., Kamolpusb, D., Gvozdenac, D., 2011. Study of operational parameters improvement of natural-gas cogeneration plant in public buildings in Thailand. *Energy Build.* 43 (4), 925–934.
- Song, J., Choi, Y., 2016. Analysis of the potential for use of floating photovoltaic systems on mine pit lakes: Case study at the Ssangyong open-pit limestone mine in Korea. *Energies* 9 (2), 1–13. <http://dx.doi.org/10.3390/en9020102>.
- Sukumaran, S., Sudhakar, K., 2017a. Fully solar powered airport: A case study of Cochin International airport. *J. Air Transp. Manage.* 62, 176–188. <http://dx.doi.org/10.1016/j.jairtraman.2017.04.004>.
- Sukumaran, S., Sudhakar, K., 2017b. Fully solar powered Raja Bhoj International Airport: A feasibility study. *Resour.-Eff. Technol.* 3 (3), 1–8. <http://dx.doi.org/10.1016/j.refitt.2017.02.001>.
- Sukumaran, S., Sudhakar, K., 2018. Performance analysis of solar powered airport based on energy and exergy analysis. *Energy* 149, 1000–1009. <http://dx.doi.org/10.1016/j.energy.2018.02.095>.
- Sundaram, S., Babu, J.S.C., 2015. Performance evaluation and validation of 5 MW grid connected solar photovoltaic plant in South India. *Energy Convers. Manage.* 100, 429–439. <http://dx.doi.org/10.1016/j.enconman.2015.04.069>.
- Tiba, C., Barbosa de, E.M.S., 2002. Softwares for designing, simulating or providing diagnosis of photovoltaic water-pumping systems. *Renew. Energy* 25 (1), 101–113. [http://dx.doi.org/10.1016/S0960-1481\(00\)00172-5](http://dx.doi.org/10.1016/S0960-1481(00)00172-5).
- United States Environmental Protection Agency, 2019. Sources of Greenhouse Gas Emissions. Retrieved November 19, 2019, from <https://www.epa.gov/ghgemissions/sources-greenhouse-gas-emissions>.
- Verma, A., Singhal, S., 2015. Solar PV performance parameter and recommendation for optimization of performance in large scale grid connected solar PV plant—case study. *J. Energy Power Sources* 2 (1), 40–53. <http://dx.doi.org/10.1186/s40807-017-0042-z>.
- Weisstein, E.W., 2019. Reflection. Retrieved December 10, 2019, from <http://mathworld.wolfram.com/Reflection.html>.
- Wikipedia, 2018. Sultan Haji Ahmad Shah international airport. Retrieved September 12, 2018, from [https://en.wikipedia.org/wiki/Sultan\\_Haji\\_Ahmad\\_Shah\\_Airport](https://en.wikipedia.org/wiki/Sultan_Haji_Ahmad_Shah_Airport).
- Wikipedia, 2019. Line plane intersection. Retrieved August 23, 2019, from [http://en.wikipedia.org/wiki/Line-plane\\_intersection](http://en.wikipedia.org/wiki/Line-plane_intersection).
- Wybo, J., 2013. Large-scale photovoltaic systems in airport areas: Safety concerns. *Renew. Sustain. Energy Rev.* 21, 402–410.